Research Article

An Improvement of Catalytic Converter Activity Using Copper Coated Activated Carbon Derived from Banana Peel

Abdul Hamid[a]* , Misbakhul Fatah[a], Wahyu Budi Utomo[a], Ike Dayi Febriana[a], Zeni Rahmawati[b], Annafiyah[a], Aurista Miftahatul Ilmah[c]

[a]Department of Heavy Equipment Mechanical Engineering, Politeknik Negeri Madura, Indonesia

[b]Department of Chemistry, Institut Teknologi Sepuluh Nopember, Indonesia

[c]Department of Ship Building Engineering, Politeknik Negeri Madura, Indonesia

Abstract. The emission of nitrogen oxide (NO_x), nitrogen monoxide (NO) and carbon monoxide (CO) from vehicle exhaust gas generates an adverse effect to the environment as well as the human health. Therefore, the need to reduce such emission is urgent. The decrease of the emission can be achieved through the use of catalytic converter. This study explains the application of catalytic converter prepared from activated carbon to enhance the activity through its adsorption ability. The activated carbon was derived from banana peels after heating them up at 400 °C for 1.5 hours and activation using natrium hydroxide (NaOH). Several techniques including N_2 adsorption-desorption, X-Ray Diffraction (XRD), Scanning Electron Microscopy-Electron Dispersive X-ray (SEM-EDX), and Fourier Transform Infrared (FTIR) were adopted to characterize the activated carbon properties. The activated carbon formed was then coated with copper. The activity of the catalytic converter using activated carbon coated with copper was then tested for its performance on diesel engine Yanmar TF 70 LY-DI with variations in the number of catalyst layers, namely 1 layer (C1), 2 layers (C2) and 3 layers (C3). Sample with three layers (C3) of catalyst exhibited the highest activity with the percentage efficiency in reducing emissions concentration of 48.76 %; 31.27 % and 29.35 % for NO_x, NO and CO, respectively.

Keywords: Catalytic converter, emission, copper, activated carbon, banana peel

1. Introduction

Exhaust gas from vehicles contribute the highest pollution to the air, and threaten the atmosphere, environment, and human health. One of the main sources of pollution that produces toxic gases is diesel-engined vehicles. Diesel engine exhaust gases were found to contain many toxic air contaminants (Sugavaneswaran *et al*., 2019). These pollutants contain numerous hazardous gases such as CO, NO_x and hydrocarbons (S. Dey & Chandra Dhal, 2020). Diesel fuel combustion specifically produces CO, NO_x, SO_x, and particulate matter (Nofendri, 2019). Unfortunately, an incomplete combustion generates a high number of such gases. Such a situation resulted in air pollution and decreased air quality to the point where it could create inconvenience and health problems (Manojkumar *et al*., 2021; Naveenkumar *et al*., 2020). The higher pollutant in the air leads to the more serious issues like greenhouse effect, acidic rain and climate change. Subsequently, there is an immense urge to resolve this challenge.

Many studies have been conducted to control the amount of NO_x and CO emission (Ghofur *et al*., 2018; Rajakrishnamoorthy *et al*., 2020). Catalytic converter was considered as the promising solution owing to its capability to transform CO and hydrocarbon into less hazardous CO_2 through redox reaction (Sugavaneswaran *et al*., 2019). A catalytic converter was commonly prepared from platinum (Kora *et al*., 2019), palladium (Abdi *et al*., 2020), zinc (Udhayakumar *et al*., 2021), aluminum (Fedotov *et al*., 2017) and copper (Manojkumar *et al*., 2021). Among those metal, copper was preferable based upon the high corrosive resistance and economic point of view.

Irawan *et al*. (Bagus Irawan *et al*., 2015) investigated the manganese-coated copper for a catalytic converter of diesel engine. The catalytic converter showed a high performance with 76% reduction of CO emission at 3000 rpm. On the other hand, the uncoated copper was reported to decrease 13% CO and 19% hydrocarbon emission (Manojkumar *et al*., 2021). Hence, modification of the catalytic converter using copper as catalyst was inevitably required. This is inline with the several studies that mentioned coating with high porosity and thermal stability material like activated carbon is an ideal option (Fuentes-Cano *et al*., 2013; Klinghoffer *et al*., 2012)

Activated carbon is carbon that has been activated chemically, physically, or both (Dada *et al*., 2022; Pullas Navarrete & de la Torre, 2022; Tonoya *et al*., 2022). This activation process produces a carbon structure with open pores (Chowdhury *et al*., 2012), a larger carbon surface area and a

* Corresponding author
Email: ahamchimie@poltera.ac.id (A. Hamid)

A.Hamid et al

Int. J. Renew. Energy Dev 2023, 12(1), 144-154

| 145

higher adsorption capacity (Black *et al.*, 2016; Sethia & Sayari, 2016). Activated carbon is widely used in various fields of water treatment (Oyim *et al.*, 2022; Soliman *et al.*, 2022), catalysts (Méndez *et al.*, 2022a), gas storage (Ramesh *et al.*, 2021), as well as the cosmetic and pharmaceutical industries (Hammani *et al.*, 2019). In addition, activated carbon is usually also used for air filtration and treatment of exhaust gases or emissions *(*Bader *et al.*, 2019; Rodríguez-Sánchez *et al.*, 2022). Activated carbon is also a porous material that can be produced from agricultural and food waste (Daouda *et al.*, 2021; Durán *et al.*, 2022; Kosheleva *et al.*, 2019; Nguyen *et al.*, 2021; Ratan *et al.*, 2018; Sujiono *et al.*, 2022). The agricultural waste such as wheat straw, corn cobs, stalks and rice husks have potential as precursors in the synthesis of activated carbon. Chemical activators and temperature pyrolysis also affect the formation of activated carbon. The reagents that are often used as chemical activators include NaOH, H_3PO_4, KOH, H_2SO_4 and $ZnCl_2$. The advantage of chemical activation is that the operating temperature and pressure conditions are relatively lower. In addition, the effect of using chemicals can increase the number of pores in the product (Adegboyega *et al.*, 2015; Geng *et al.*, 2014). Meanwhile, the pyrolysis temperature required for the formation of activated carbon is between 400−900 °C. In addition, several other literatures report that the activation temperature has an important role to develop the porosity and surface functional groups obtained on activated carbon (Kosheleva *et al.*, 2019; Tripathi *et al.*, 2016). The porosity of activated carbon is mostly microporous (<2 nm) and mesoporous (2-50 nm) (Foong *et al.*, 2020). Lu and Li (Lu & Li, 2019) have conducted an analysis related to the porosity of activated carbon from banana peels. The results obtained that the average pore diameter and total pore volume were 2.11 nm and 0.32 cm^3/g. The formation of porosity from the converting banana peels into activated carbon is influenced by chemical activation (Jain *et al.*, 2016).

Many carbon applications including catalyst and adsorbent used activated carbon made from natural resources due to several considerations: the high availability and low price, and the utilization of waste to the added value material. Besides, activated carbon can reduce harm to the environment and human health compared to synthetic catalysts (Frazier *et al.*, 2015). Activated carbon can also be obtained from fruit peels (Jothi Ramalingam *et al.*, 2020). Banana peel is one of the abundant waste with high carbon and can be transformed to activated carbon through feasible method such as heating at 400 −500 °C. Khairiah *et al.* (Khairiah *et al.*, 2021) have reported that the elemental content (% wt) of activated carbon derived from banana peels is the most dominant, namely carbon and oxygen of 78.15 and 10.52 %, respectively. Borhan *et al.* (Borhan *et al.*, 2015) also analyzed the content of activated carbon from banana peels using SEM-EDX. The results showed that the elemental content (% wt) of carbon and oxygen found in the activated carbon samples from banana peels were 60.18 and 25.19 %, respectively. This indicates that banana peel waste is able to become prospective activated carbon because it has a carbon content in the range of 50 – 80 % (Borhan *et al.*, 2015). In Madura Island, banana peels could be utilized as exhaust gas adsorbent for a whole year. The present study aims to use of banana peel as the source of activated carbon. The addition of activated carbon of banana peel is expected to enhance the adsorption capacity of catalytic converter to lower the hazardous gas emission, as well as increase the strength and thermal stability. In addition, the influence of the catalyst layer was also investigated for the purpose of optimization.

2. Materials and Methods

2.1 Materials and tools

The materials used in this study include banana peel waste which originated from Madura Island, Indonesia. Activator NaOH was purchased from Merck, cassava starch was obtained locally, demineralized water, stainless steel plate and copper plate. The tools used in this research include single cylinder diesel engine Yanmar TF 70 LY-DI, tachometer, oven, drilling machine, electric welding, grinder, furnace, beaker glass, hotplate stirrer and gas analyzer.

2.2 Methods

2.2.1 Activated carbon preparation

Synthesis of activated carbon following the research conducted by Neolaka *et al.* (Neolaka *et al.*, 2021). Banana peels were cut into small pieces and dried under sunlight to remove the moisture. Carbon was achieved after the calcination of dried banana peels at 400 °C for 1.5 hours. Afterwards, carbon was crushed and sieved using 150-mesh. The activation of banana peel carbon was carried out by adding of NaOH 3 M under stirring condition at 600 rpm for 2 hours. This activation was followed by washing it with demineralized water to reach neutral pH value. To remove the water, activated carbon was dried in the oven at 110 °C for 2 hours. This procedure is illustrated in Figure 1.

2.2.2 Activated carbon characterization

The crystallinity and identification phase of activated carbon were carried out by powder X-Ray diffraction (XRD) using a Bruker D2 Phaser with Cu-Kα radiation. The diffractograms were collected at 40 kV and 40 mA, and in steps of 0.05 over the range of 5°< 2θ< 80°. The morphology and elemental content of activated carbon were analysed using Scanning Electron Microscopy-Energy Dispersive X-Ray (SEM-EDX) by Instrument Phenom Desktop. The functional group was studied by Fourier Transform Infrared (FTIR) Nicolet Avtar 360 IR. The porosity of activated carbon was determined by nitrogen adsorption using a Quantachrome Novatouch Lx4.

2.2.3 The preparation of catalytic converter using activated carbon coated with copper

The design of the catalytic converter was depicted in figure 2. The Activated carbon formed was then coated with copper like a sandwich as shown in the Figure 2. The catalyst (copper coated activated carbon) was drilled to form a hole and then covered in stainless steel chase. As for the overall dimensions of the catalytic converter, it is shown in Figure 3.

2.2.4 Catalytic converter activity

The activity of the catalytic converter was tested in an engine diesel Yanmar TF 70 LY-DI equipped with a gas analyzer (Figure 4). The performance was defined by the decrease of CO, NO, and NO_x emission. The analysis was conducted over varied catalytic converter including without catalyst (WC), one layer of catalyst (C1), two layers of catalyst (C2), and three layers of catalysts (C3). The percentage of efficiency of gas emission was formulated as follows,

$$\% \, Efficiency = \frac{C \, in - C cov}{C \, in} \, x \, 100 \, \% \qquad (1)$$

C_{in} represents emission gas concentration without a catalytic converter, and C_{cov} with catalytic converter

A.Hamid et al

Int. J. Renew. Energy Dev 2023, 12(1), 144-154

| 146

Bananas were obtained from the Madura region, Indonesia

Banana peels were dried under sunlight

Banana peels were carbonized at 400 ° C for 1.5 hours using a furnace

The sample was filtered using filter paper and washed with aquademin until the pH was neutral

The sample was activated using NaOH 3 M by stirring for 2 hours at room temperature with 600 rpm

The sample was sieved using a 150-mesh sieve

The sample was heated at 110 ºC for 2 hours using an oven

Activated carbon sample from banana peel waste

Fig. 1 Preparation of activated carbon from banana peel waste

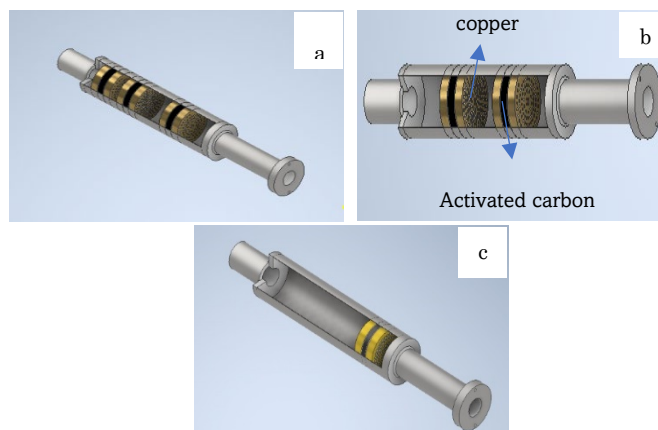**Fig. 2** Catalytic converter design with three catalysts (a), two catalysts (b), and one catalyst (c)
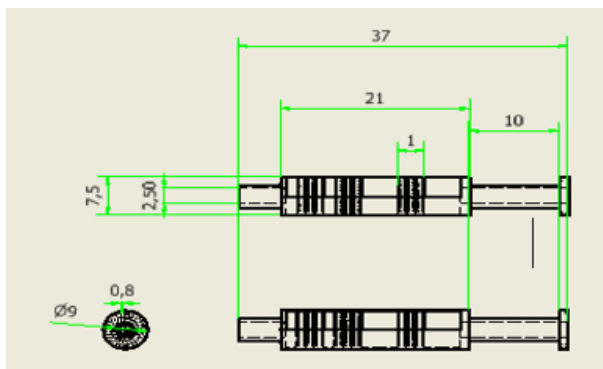
A.Hamid et al   Int. J. Renew. Energy Dev 2023, 12(1), 144-154

| 147

Fig. 3 Catalytic converter dimension
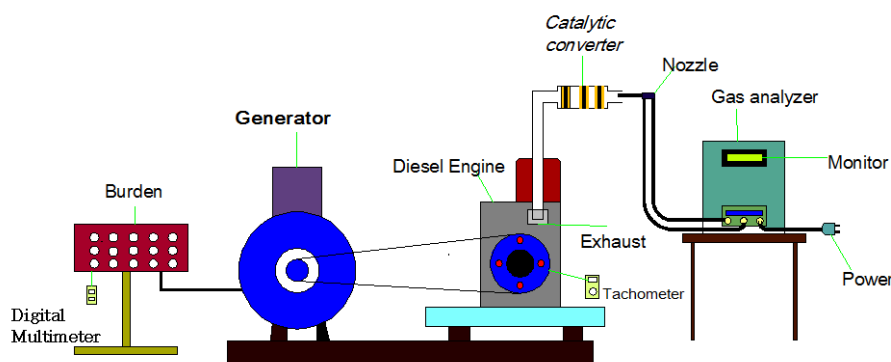

Fig. 4 Diesel engine and catalytic converter set up

3.   Results and Discussion

3.1 Activated carbon characterization

Analysis using XRD was used to determine the phase of the activated carbon sample from banana peel waste. Activated carbon samples were analysed with 2θ between 5°-80° using Cu-Kα radiation. Figure 5 describes the diffractogram of activated carbon from banana peels. The presence of carbon was confirmed by peaks at 2θ = 26.81° and 32.07°. These features also confirmed amorphous phase of activated carbon. The activated carbon showed a widening diffractogram peak at 2θ between $10° - 30°$. These peaks are the characteristic of porous materials with good porosity (Neme *et al.*, 2022).
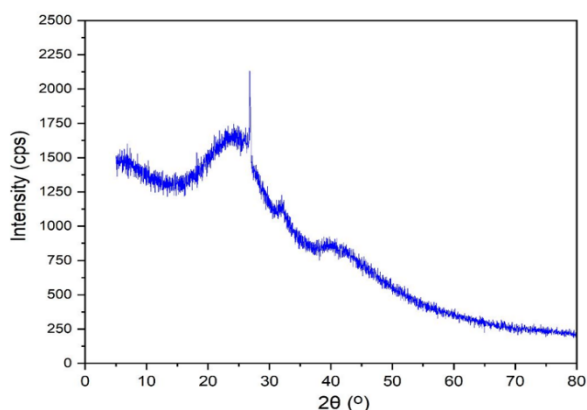

Fig. 5 Diffractogram of activated carbon from banana peels

Microstructure data of activated carbon samples using XRD analysis based on data parameters 2θ, crystal size (Å), intensity and FWHM (Full-Width at Half Maximum) are shown in Table 1. The data were obtained from the two highest peaks in activated carbon samples from banana peels. The first peak at 2θ = 26.81° with crystal size of 3.32 Å, FWHM value at 0.18530°, and intensity at 2130 cps. The second highest peak at 2θ = 32.07° with a crystal size of 2.79 Å, FWHM value is 0.333° and intensity is 1164 cps. The FWHM value provides information about the crystalline homogeneity of the synthesized activated carbon. Good material quality was indicated by the relatively smaller FWHM value in accordance with the sample crystal structure and homogeneous lattice (Sujiono *et al.*, 2020).

The morphology and EDX spectrum of activated carbon is illustrated in Figure 6 and 7. The micrographs showed irregular sheet-like and rough surface with particle size about 30 μm. Some pores and structural channels were also examined. Table 2 shows that the highest elemental contents of activated carbon based on EDX results, namely carbon and oxygen, were obtained at 78.36 and 18.50 %, respectively.

Table 1
XRD data of two highest peaks of activated carbon

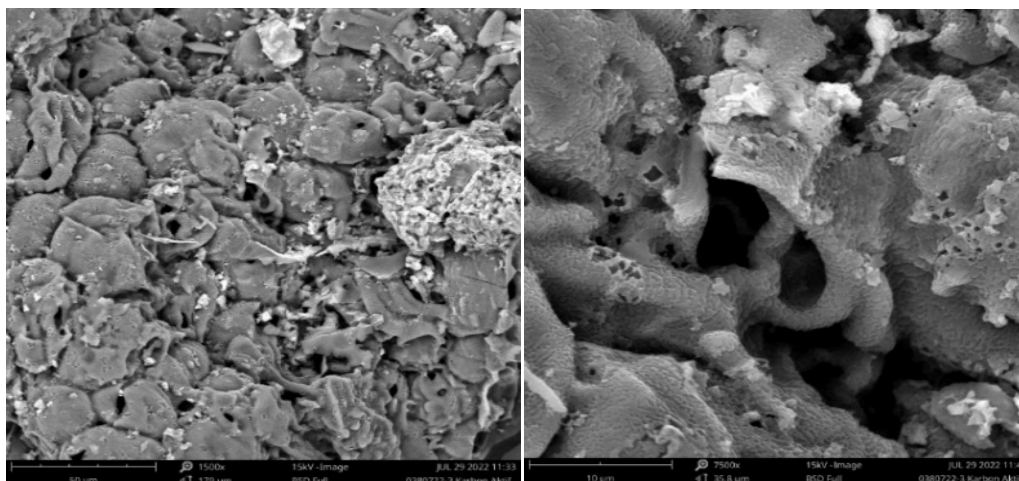| 2θ (°)	d (Å)	Intensity (cps)	FWHM (°)
26.81	3.32	2130	0.187
32.07	2.79	1164	0.333

A.Hamid et al

Int. J. Renew. Energy Dev 2023, 12(1), 144-154

| 148

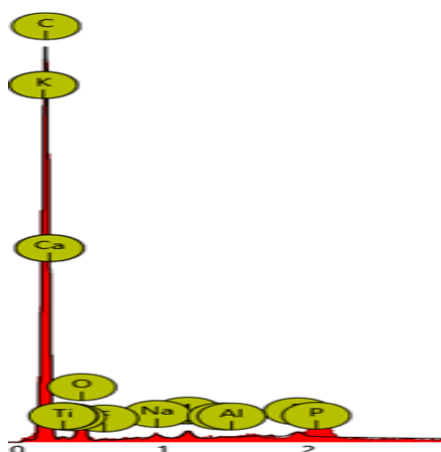**Fig. 6** Morphology of activated carbon from banana peels

Fig. 7 EDX spectrum of activated carbon from banana peels

Table 2

The composition of activated carbon analyzed by EDX

Element	Elemental Content (%)
Carbon	78.36
Oxygen	18.50
Calcium	0.82
Magnesium	0.75
Fluorine	0.53
Phosphorous	0.45
Sodium	0.43
Potassium	0.10
Aluminum	0.08
Titanium	0

The nitrogen adsorption-desorption isotherm of activated carbon from banana peels is shown in Figure 8a. In this figure, it can be seen that the nitrogen adsorption-desorption isotherm of activated carbon occured in the adsorption of high amounts of nitrogen molecules at a relative pressure of P/P_0 of zero to relative pressure of P/P_0 was 0.2. Then, there was a slight increase in the volume of nitrogen molecules adsorbed at a higher relative pressure P/P_0 ($P/P_0 > 0.3$) which indicated the occurrence of mesoporous filling. The solid surface would be covered by nitrogen molecules to form a single layer (monolayer). The presence of pores on the solid surface would have the effect of limiting the number of layers on the adsorbate and the phenomenon of capillary condensation occurs (Nugraha *et al.*, 2021). This capillary condensation would cause hysteresis. Hysteresis loops could occur due to incomplete condensation resulting in a metastable adsorption phase (Carraro *et al.*, 2019). In Figure 8a, a hysteresis loop was observed during desorption at a relative pressure of P/P_0 0.4-1. Based on the pattern of nitrogen adsorption- desorption above, it can be generally concluded that activated carbon shows a type IV adsorption profile which is characteristic of meso-sized pore solids with the size of 2-50 nm as presented by the pore size distribution in Figure 8b. The activated carbon sample showed meso-sized pores with the observed peak of the pore size distribution at a pore diameter of about 2-4 nm to be exact at 3.1 nm.

The functional group of activated carbon was investigated by FTIR, as described in Figure 9. FTIR characterization of activated carbon samples recorded at wave numbers between 500 to 4000 cm^{-1}. The FTIR spectra of activated carbon samples showed several peaks at 3387, 1580, 1378 and 1035 cm^{-1}. The presence of hydroxyl group was confirmed by the broad peak at 3387 cm^{-1}, as a result of the reaction between NaOH and carbon on the surface (Rawal *et al.*, 2018; Soleimani & Kaghazchi, 2014; Waly *et al.*, 2021). The peak observed at 1580 cm^{-1} is the C=O stretching vibration which was associated with the carboxylic acid (Freitas *et al.*, 2019; Li *et al.*, 2019). The sharp peaks at 1378 cm^{-1} assigned the vibration of C=C bonding from aromatic ring and the indication of carbon activation by NaOH (S. Zhang *et al.*, 2013). The feature at 1035 and 875 cm^{-1} represented the vibration of C-O group and C-H aromatic, respectively (Saleh, 2018; Tran *et al.*, 2023).
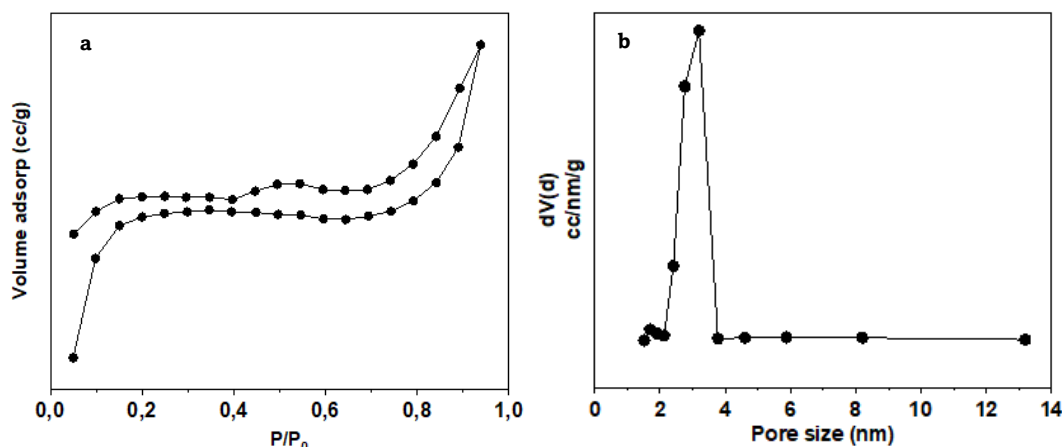
A.Hamid et al

Int. J. Renew. Energy Dev 2023, 12(1), 144-154

| 149

Fig. 8 Nitrogen adsorption-desorption isotherm (a) and pore size distribution (b) of activated carbon
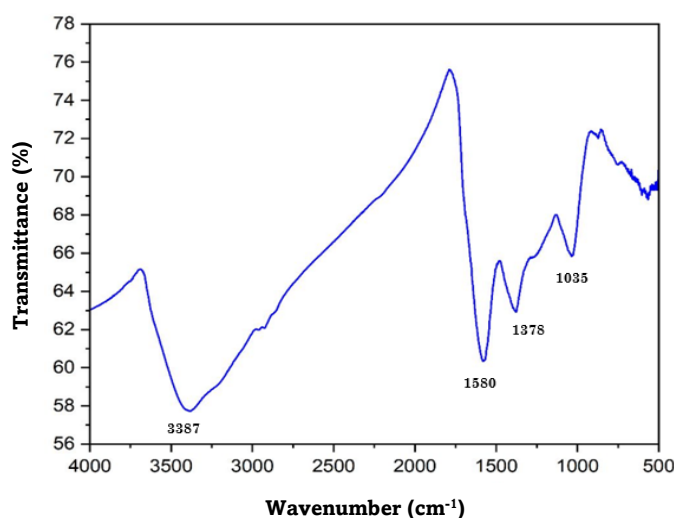

Fig. 9 FTIR spectra of activated carbon from banana peels

The characterization results of activated carbon using FTIR in the study are the same as the research conducted by Neolaka *et.al*, Rawal *et.al*, and Mendez *et.al.* (Méndez *et al*., 2022b; Neolaka *et al*., 2021; Rawal *et al*., 2018). O–H and and C–O stretching vibrations obtained from activated carbon samples play an important role as pollutant absorbers (Shu *et al*., 2017). The absorption of particles in the use of a catalyst is also occurs due to the presence of functional groups containing oxygen atoms on the surface of sample (Li *et al*., 2019).
.

3.1 Catalytic converter activity

The catalytic converter was tested in diesel engine with the alteration of speed in the range of 100-1500 rpm within 100 intervals. Aside from that, the catalyst layers were also varied for the optimization process. The result was rationalized by the efficiency percentage of NO, NOₓ and CO. The activity of catalytic converter on the NO and NOₓ emission tests is described in Figure 10 and 11. The nitrogen oxide was formed by the reaction between oxygen and nitrogen from air at high temperature during the combustion of the fuel as mentioned in scheme 2 (Ilkiliç, 2009). Aside from the combustion, the fuel contained nitrogen oxide (NO_x). Overall, the application of catalytic converter decreased the emission of NO. Unsurprisingly, the highest NO emission was generated by the absence of catalytic converter with 201 ppm at 1100 rpm. In contrast, the lowest NO emission of 134 ppm at 1300 rpm was

exhibited from the application of three layers of catalyst (C3). More layers of catalyst provided sufficient active sites to accommodate the reduction of NO_x to N_2. Moreover, the presence of activated carbon leads to more adsorption of exhaust gases.

Generally, the NO emission depleted as the engine speed increased over catalytic converter C2 and C3. However, the emission rose when the rotation was 1300 rpm. Similar trend was also observed in Figure 11. This phenomenon occurred owing to the complete combustion at 1300. Afterwards, the emission then continuously increased due to the higher supply of air at high rotation of the engine.

The highest NO_x emission test results were obtained without using a catalytic converter, which was 211 ppm at 1100 rpm. Meanwhile the lowest NO_x emission gas content was attained when using a catalytic converter with three catalysts (C3), namely 140 ppm at 1300 rpm. This showed that the more the number of catalysts used, the lower the gas emission content produced from the diesel engine. NO_x formation was influenced by the flash point, combustion duration and oxygen concentration (Kataria *et al*., 2019). The reduction process occurs in the presence of a copper metal catalyst coated with activated carbon. Gases such as NO and NO_x are reduced from the catalytic converter.
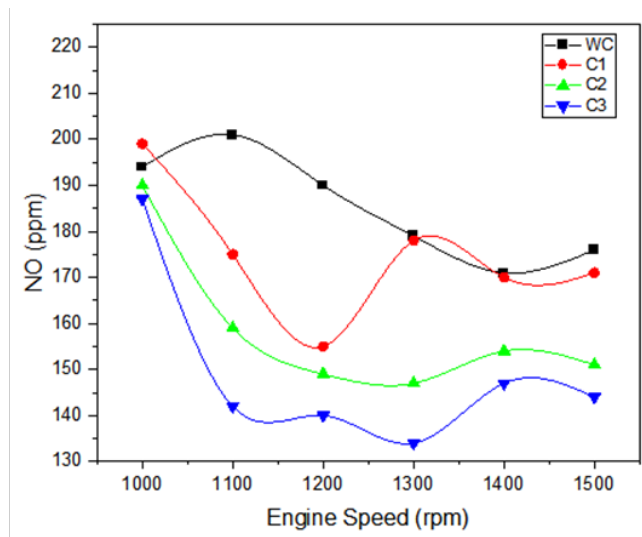
$$NO_x \rightarrow N_2 + O_2 \qquad (2)$$

A.Hamid et al

Int. J. Renew. Energy Dev 2023, 12(1), 144-154
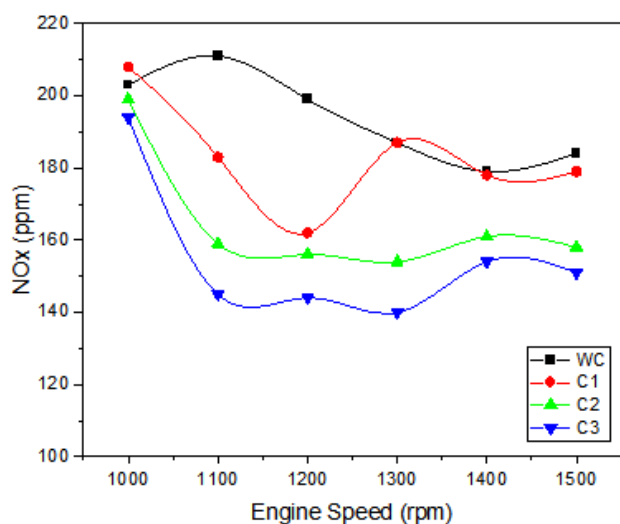
| 150

Fig. 10 The emission of NO

Fig. 11 The emission of NO_x

Figure 12 describes the comparison of CO emission of exhaust gas resulting from the engine with the presence and absence of catalytic converter. The use of catalytic converter mainly resulted in lower CO emission. The highest was resulted from combustion over the WC sample, with 484 ppm at 1100 rpm. Conversely, the lowest emission of 304 ppm at 1300 rpm was produced from sample C3 with three layers of catalyst.

Carbon monoxide was generated by the incomplete combustion of hydrocarbon in the combustion chamber (Ganesan *et al.*, 2021). The high performance of copper metal was associated with the presence of intra and inter-particle porosity in the catalyst and high dispersion of copper particles on the catalyst surface (Subhashish Dey & Dhal, 2019). The number of oxygen species adsorbed on the surface of copper played an important role for the catalytic conversion of CO emission. In such a manner, the CO emission content produced after passing through the catalyst of activated carbon coated with copper decreases. The catalytic converter captured the CO molecules to enable the oxidation proceeded. The oxidation reaction for the formation of CO emission is an exothermic reaction, especially a catalyst combustion reaction which is better known as catalytic oxidation reaction. If there is not enough oxygen in the air, incomplete combustion will occur so that the carbon in the fuel will produce CO emission gas. The metal catalyst alloyed with copper and activated carbon will

accelerate the gas reaction by forming weak bonds between the gas and metal atoms on the surface of the catalyst. So that the catalytic converter using activated carbon coated with copper is able to convert harmful pollutants such as CO emission gas to be converted into CO_2. Eventually, the CO was converted to less hazardous CO_2 and released to the air. The presence of copper coated activated carbon which has high porosity and excellent metal dispersion could enhance the oxidation process. The CO emission declined as the engine rotation increased to 1300. At this point, complete combustion had taken place.

Compared to CO and NO, the highest CO_2 emission was produced from C3 samples, as illustrated in Figure 13. The CO_2 was produced by two processes, the result of hydrocarbon combustion and the oxidation of CO on the catalytic converter. Subsequently, CO_2 emission trend differed from NO and CO emission. Figure 13 also presents that the highest CO_2 emission content is obtained at C2 and C3, which is 2.7 % at 1500 rpm, while the lowest CO_2 emission content is obtained in the WC is 2 % at 1000 rpm. The engine speed significantly affected the formation of CO_2. Such high speed permitted more air to the combustion chamber and provided more oxygen for fuel combustion (Abed *et al.*, 2018). The susceptible mole ratio of oxygen-hydrocarbon created a complete combustion and produces more CO_2. The reaction of CO_2 production is mentioned in the following scheme 3 (Jeyakumar *et al.*, 2020).
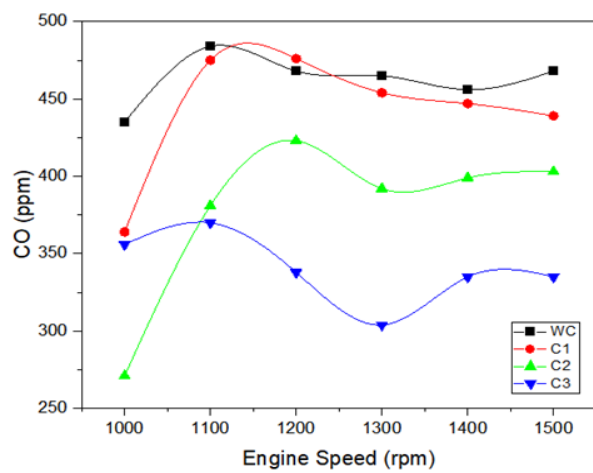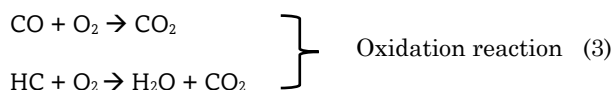
$$CO + O_2 \rightarrow CO_2$$

$$HC + O_2 \rightarrow H_2O + CO_2$$

Oxidation reaction   (3)

Fig. 12 The emission of CO

Fig. 13 The emission of CO_2

A.Hamid et al   Int. J. Renew. Energy Dev 2023, 12(1), 144-154
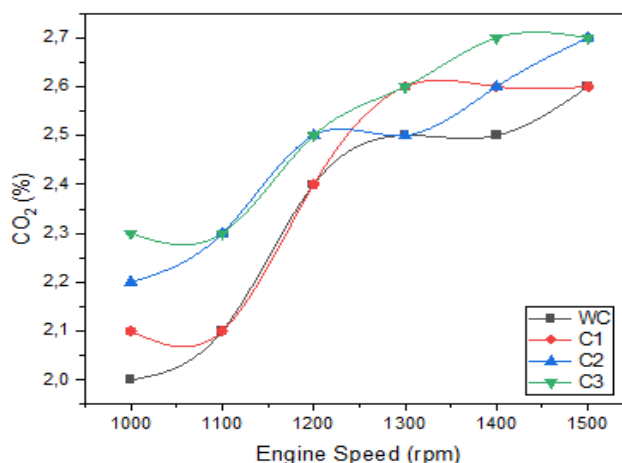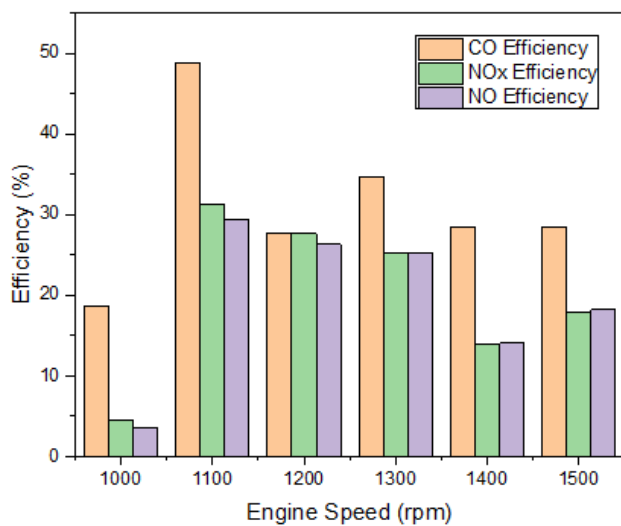
| 151

Fig. 14 The efficiency of CO, NO$_x$ and NO emission over catalytic converter with three layers of catalyst (C3)

The emission of each gas over C3 samples was profoundly analyzed in depth regarding how much efficiency the reduction of CO, NO$_x$ and NO emissions, as shown in Figure 14. In terms of engine speed, the emission of all gasses declined as the function rotated. Higher speed also produced more combustion and consumed more fuel. Therefore, the emission also reached higher. Regarding the catalyst layers, the higher number of catalysts lowered the gas emission efficiency. Catalysts provided more active sites to accommodate exhaust gas and transformed them to less dangerous gasses. Nevertheless, to a certain degree the adsorption reached maximum level when the active sites were covered with the gases. This phenomenon was followed by the gas desorption caused by the weakened interaction (Huang *et al.*, 2014). This indicated that the adsorption rate and mechanism were affected by the physical electrostatic force (Nikić *et al.*, 2019; G. Zhang *et al.*, 2009). Figure 14 also shows that the efficiency rate declined was

reached at 1100 rpm with the following numbers CO: 48.76 %, NO$_x$: 31.27 % and NO: 29.35 %.

Table 3 shows the comparison of results from several previous studies regarding catalytic converters for diesel engine with different types of catalyst. The use of catalysts that have adsorption capabilities on emissions from diesel engines shows a very effective performance. The highest efficiency of reducing CO emission concentration is using Co-ZSM-5 Zeolites as catalyst. Zeolite-based catalytic converter has better performance. Based on research that has been carried out by Rajakrishnamoorthy *et al.* (Rajakrishnamoorthy *et al.*, 2020), the concentration of CO emissions was significantly reduced at all levels of load conditions using Co-ZSM-5 zeolites as catalyst. The use of zeolite-based catalysts such as natural zeolite is also able to reduce the concentration of SO$_2$ emissions up to 94% (Hamid & Wilujeng, 2021). The highest NO$_x$ emission reduction efficiency was obtained using a copper oxide catalyst (Venkatesan *et al.*, 2017). The NO$_x$ compound was significantly decreased when the engine was left running with the catalytic converter at all loads. The results revealed that the reduction efficiency of NO$_x$ emission concentration is 61 % at full load. The manufacture of the catalytic converter in this study uses a combination of materials that can reduce gas emissions through absorption and materials with catalytic properties, although most studies still classify metal filters for catalytic converters into several elements such as copper, titanium, and aluminium. The expected advantage by combining these two properties is the creation of an optimal material that can reduce gas emissions from diesel engine. In addition, all the supporting materials for making the catalytic converter in this study came from Indonesia with easy availability and low cost. In such a manner, the combination of copper coated activated carbon can reduce CO and NO$_x$ emissions by around 49 and 31 %. The activating group on the surface of activated carbon can interact as an adsorption media because it has a porous crystal structure and high thermal stability. The catalytic converter in this study is effective to decrease the concentration of emissions from diesel engine when compared to the previous studies.

Table 3
Comparison of previous research related to catalytic converters

No	Catalysts used in catalytic converter	Emission reduction efficiency value			Reference
1	Silicon dioxide and alumina	CO: 33 %	HC: 83 %		(Arunkumar *et al.*, 2016)
2	Cu-ZSM-5 Zeolites	CO: 87 %	NO: 56 %	HC: 80 %	(Rajakrishnamoorthy *et al.*, 2020)
	Co-ZSM-5 Zeolites	CO: 88 %	NO$_x$: 59 %	HC: 79 %	
3	Natural zeolites	CO: 42 %	SO$_2$: 94 %		(Hamid & Wilujeng, 2021)
4	Activated charcoal	CO: 33 %	NO$_x$: 13 %	HC: 36 %	(Naveenkumar *et al.*, 2020)
5	Aluminum oxide and titanium dioxide	CO: 50 %	HC: 58 %		(Vembathu Rajesh *et al.*, 2020)
6	Activated carbon from banana hump	CO: 25 %	NO$_x$: 27 %	HC: 20 %	(Presin Kumar *et al.*, 2019)
7	Copper oxide	CO: 21 %	NO$_x$: 61 %	HC: 32 %	(Venkatesan *et al.*, 2017)
8	Fly ash	CO: 34 %	HC: 32 %		(Ghofur *et al.*, 2018)
9	Copper coated activated carbon	CO: 49 %	NO$_x$: 31 %	NO: 29 %	This research

A.Hamid et al

Int. J. Renew. Energy Dev 2023, 12(1), 144-154

| 152

4. Conclusion

A catalytic converter was successfully prepared from activated carbon from banana peel coated with copper. The FTIR confirmed the potential utility of activated carbon for exhaust gas adsorption with the carboxyl and hydroxyl functional group. Diffractogram affirmed the porous phase and low crystallinity of activated carbon. The uniformly porous surface was verified by SEM-EDX, as well as the presence of carbon and oxygen as the main elements. In line with the finding, analysis using nitrogen adsorption-desorption showed the presence of meso-sized pores. The application of activated carbon in catalytic converter could decline gas emission, which decreased along with the amount of catalyst layers. The highest efficiency was obtained from C3 samples at 1100 rpm with the following efficiency value CO: 48.76 %, NO_x: 31.27 % and NO: 29.35 %.

Author Contributions: AH: Supervised the study, acquired funding, conceptualization, reviewed and edited the manuscript, WBU: performed the experiments and data analysis, MF: performed the experiments and data analysis, resources projects, IDF: project administration and editing, ZR: supervision, writing—review, A: reviewed and edited the manuscript, AMI: writing—review, editing and validation. All authors have read and agreed to the published version of the manuscript

Conflicts of Interest: The authors declare no conflict of interest

References

Abdi, K., Ezoddin, M., & Pirooznia, N. (2020). Temperature-controlled liquid–liquid microextraction using a biocompatible hydrophobic deep eutectic solvent for microextraction of palladium from catalytic converter and road dust samples prior to ETAAS determination. *Microchemical Journal*, *157*(May), 104999. https://doi.org/10.1016/j.microc.2020.104999

Abed, K. A., El Morsi, A. K., Sayed, M. M., Shaib, A. A. E., & Gad, M. S. (2018). Effect of waste cooking-oil biodiesel on performance and exhaust emissions of a diesel engine. *Egyptian Journal of Petroleum*, *27*(4), 985–989. https://doi.org/10.1016/j.ejpe.2018.02.008

Adegboyega, S. O., Olusegun, A. A., Michael, S. O., Mku, T. I., & Sam, S. A. (2015). Preparation of phosphoric acid activated carbons from Canarium Schweinfurthii Nutshell and its role in methylene blue adsorption. *Journal of Chemical Engineering and Materials Science*, *6*(2), 9–14. https://doi.org/10.5897/jcems2015.0219

Arunkumar, S., Kankeyan, M., Muneeswaran, V., & Aravind, M. R. (2016). *Exhaust Emission Reduction in SI Engine Using Catalytic Converter With Silicon Dioxide & Alumina With Silica as Catalysts*. *2*, 72–78.

Bader, N., Sager, U., Schneiderwind, U., & Ouederni, A. (2019). Foam and granular olive stone-derived activated carbons for NO2 filtration from indoor air. *Journal of Environmental Chemical Engineering*, *7*(2), 103005. https://doi.org/10.1016/j.jece.2019.103005

Bagus Irawan, R., Purwanto, P., & Hadiyanto, H. (2015). Optimum Design of Manganese-coated Copper Catalytic Converter to Reduce Carbon Monoxide Emissions on Gasoline Motor. *Procedia Environmental Sciences*, *23*(Ictcred 2014), 86–92. https://doi.org/10.1016/j.proenv.2015.01.013

Black, R., Equilibrium, D., Studies, K., Mook, W. T., Aroua, K., & Szlachta, M. (2016). *Palm Shell-based Activated Carbon for Removing*. *11*(1), 1432–1447.

Borhan, A., Thangamuthu, S., Taha, M. F., & Ramdan, A. N. (2015). Development of activated carbon derived from banana peel for CO2 removal. *AIP Conference Proceedings*, *1674*. https://doi.org/10.1063/1.4928819

Carraro, P. S., Spessato, L., Crespo, L. H. S., Yokoyama, J. T. C., Fonseca, J. M., Bedin, K. C., Ronix, A., Cazetta, A. L., Silva, T. L., & Almeida, V. C. (2019). Activated carbon fibers prepared from cellulose and polyester–derived residues and their application on removal of Pb2+ ions from aqueous solution. *Journal of Molecular Liquids*, *289*, 111150. https://doi.org/10.1016/j.molliq.2019.111150

Chowdhury, Z. Z., Zain, S. M., Khan, R. A., Rafique, R. F., & Khalid, K. (2012). Batch and fixed bed adsorption studies of lead (ii) cations from aqueous solutions onto granular activated carbon derived from mangostana garcinia shell. *BioResources*, *7*(3), 2895–2915.

Dada, A. O., Inyinbor, A. A., Tokula, B. E., Bello, O. S., & Pal, U. (2022). Preparation and characterization of rice husk activated carbon-supported zinc oxide nanocomposite (RHAC-ZnO-NC). *Heliyon*, *8*(8), e10167. https://doi.org/10.1016/j.heliyon.2022.e10167

Daouda, M. M. A., Akowanou, A. V. O., Mahunon, S. E. R., Adjinda, C. K., Aina, M. P., & Drogui, P. (2021). Optimal removal of diclofenac and amoxicillin by activated carbon prepared from coconut shell through response surface methodology. *South African Journal of Chemical Engineering*, *38*(July), 78–89. https://doi.org/10.1016/j.sajce.2021.08.004

Dey, S., & Chandra Dhal, G. (2020). Controlling carbon monoxide emissions from automobile vehicle exhaust using copper oxide catalysts in a catalytic converter. *Materials Today Chemistry*, *17*, 100282. https://doi.org/10.1016/j.mtchem.2020.100282

Dey, S., & Dhal, G. C. (2019). Materials progress in the control of CO and CO2 emission at ambient conditions: An overview. *Materials Science for Energy Technologies*, *2*(3), 607–623. https://doi.org/10.1016/j.mset.2019.06.004

Durán, I., Rubiera, F., & Pevida, C. (2022). Modeling a biogas upgrading PSA unit with a sustainable activated carbon derived from pine sawdust. Sensitivity analysis on the adsorption of CO2 and CH4 mixtures. *Chemical Engineering Journal*, *428*. https://doi.org/10.1016/j.cej.2021.132564

Fedotov, A. S., Antonov, D. O., Bukhtenko, O. V., Uvarov, V. I., Kriventsov, V. V., & Tsodikov, M. V. (2017). The role of aluminum in the formation of Ni–Al–Co-containing porous ceramic converters with high activity in dry and steam reforming of methane and ethanol. *International Journal of Hydrogen Energy*, *42*(38), 24131–24141. https://doi.org/10.1016/j.ijhydene.2017.07.095

Foong, S. Y., Liew, R. K., Yang, Y., Cheng, Y. W., Yek, P. N. Y., Wan Mahari, W. A., Lee, X. Y., Han, C. S., Vo, D. V. N., Van Le, Q., Aghbashlo, M., Tabatabaei, M., Sonne, C., Peng, W., & Lam, S. S. (2020). Valorization of biomass waste to engineered activated biochar by microwave pyrolysis: Progress, challenges, and future directions. *Chemical Engineering Journal*, *389*(February), 124401. https://doi.org/10.1016/j.cej.2020.124401

Frazier, R. S., Jin, E., & Kumar, A. (2015). Life cycle assessment of biochar versus metal catalysts used in syngas cleaning. *Energies*, *8*(1), 621–644. https://doi.org/10.3390/en8010621

Freitas, J. V., Nogueira, F. G. E., & Farinas, C. S. (2019). Coconut shell activated carbon as an alternative adsorbent of inhibitors from lignocellulosic biomass pretreatment. *Industrial Crops and Products*, *137*(May), 16–23. https://doi.org/10.1016/j.indcrop.2019.05.018

Fuentes-Cano, D., Gómez-Barea, A., Nilsson, S., & Ollero, P. (2013). Decomposition kinetics of model tar compounds over chars with different internal structure to model hot tar removal in biomass gasification. *Chemical Engineering Journal*, *228*, 1223–1233. https://doi.org/10.1016/j.cej.2013.03.130

Ganesan, S., Mohanraj, M., Guruprakaash, R., & Logeshwar, S. (2021). Impact of bamboo and castor composite catalytic converter on VCR diesel engine emission using Wheat germ oil. *Materials Today:Proceedings*. https://doi.org/10.1016/j.matpr.2021.03.680

Geng, Z., Wang, D., Zhang, C., Zhou, X., Xin, H., Liu, X., & Cai, M. (2014). Spillover enhanced hydrogen uptake of Pt/Pd doped corncob-derived activated carbon with ultra-high surface area at

A.Hamid et al

Int. J. Renew. Energy Dev 2023, 12(1), 144-154

| 153

high pressure. *International Journal of Hydrogen Energy*, *39*(25), 13643–13649. https://doi.org/10.1016/j.ijhydene.2014.02.065

Ghofur, A., Soemarno, Hadi, A., & Putra, M. D. (2018). Potential fly ash waste as catalytic converter for reduction of HC and CO emissions. *Sustainable Environment Research*, *28*(6), 357–362. https://doi.org/10.1016/j.serj.2018.07.003

Hamid, A., & Wilujeng, A. D. (2021). *The Reduction of CO and SO 2 by Natural Zeolites in Catalytic Converter of Diesel Engine*. *208*(Icist 2020), 162–167.

Hammani, H., Laghrib, F., Farahi, A., Lahrich, S., El Ouafy, T., Aboulkas, A., El Harfi, K., & El Mhammedi, M. A. (2019). Preparation of activated carbon from date stones as a catalyst to the reactivity of hydroquinone: Application in skin whitening cosmetics samples. *Journal of Science: Advanced Materials and Devices*, *4*(3), 451–458. https://doi.org/10.1016/j.jsamd.2019.07.003

Huang, Y., Li, S., Chen, J., Zhang, X., & Chen, Y. (2014). Adsorption of Pb(II) on mesoporous activated carbons fabricated from water hyacinth using H 3 PO 4 activation: Adsorption capacity, kinetic and isotherm studies. *Applied Surface Science*, *293*, 160–168. https://doi.org/10.1016/j.apsusc.2013.12.123

Ilkiliç, C. (2009). Emission characteristics of a diesel engine fueled by 25% sunflower oil methyl ester and 75% diesel fuel blend. *Energy Sources, Part A: Recovery, Utilization and Environmental Effects*, *31*(6), 480–491. https://doi.org/10.1080/15567030701531329

Jain, A., Balasubramanian, R., & Srinivasan, M. P. (2016). Hydrothermal conversion of biomass waste to activated carbon with high porosity: A review. *Chemical Engineering Journal*, *283*, 789–805. https://doi.org/10.1016/j.cej.2015.08.014

Jeyakumar, N., Arumugam, C. A. K., Narayanasamy, B., & Rajkumar, R. (2020). Effect of wash coat layers on the conversion efficiency of a catalytic converter in the SI engine. *International Journal of Ambient Energy*, *0*(0), 1–27. https://doi.org/10.1080/01430750.2020.1712256

Jothi Ramalingam, R., Sivachidambaram, M., Vijaya, J. J., Al-Lohedan, H. A., & Muthumareeswaran, M. R. (2020). Synthesis of porous activated carbon powder formation from fruit peel and cow dung waste for modified electrode fabrication and application. *Biomass and Bioenergy*, *142*(October), 105800. https://doi.org/10.1016/j.biombioe.2020.105800

Kataria, J., Mohapatra, S. K., & Kundu, K. (2019). Biodiesel production from waste cooking oil using heterogeneous catalysts and its operational characteristics on variable compression ratio CI engine. *Journal of the Energy Institute*, *92*(2), 275–287. https://doi.org/10.1016/j.joei.2018.01.008

Khairiah, K., Frida, E., Sebayang, K., Sinuhaji, P., & Humaidi, S. (2021). Data on characterization, model, and adsorption rate of banana peel activated carbon (Musa Acuminata) for adsorbents of various heavy metals (Mn, Pb, Zn, Fe). *Data in Brief*, *39*, 107611. https://doi.org/10.1016/j.dib.2021.107611

Klinghoffer, N. B., Castaldi, M. J., Nzihou, A., Klinghoffer, N. B., Castaldi, M. J., Nzihou, A., Properties, C., Perfor-, C., Klingho, N. B., Castaldi, M. J., & Nzihou, A. (2012). Catalyst Properties and Catalytic Performance of Char from Biomass Gasification. *Industrial and Engineering Chemistry Research*, *51*(40), 13113–13122.

Kora, A. J., Madhavi, K., Meeravali, N. N., & Jai Kumar, S. (2019). In situ synthesis and preconcentration of cetylpyridinium complexed hexaiodo platinum nanoparticles from spent automobile catalytic converter leachate using cloud point extraction. *Arabian Journal of Chemistry*, *13*(3), 4594–4605. https://doi.org/10.1016/j.arabjc.2019.10.008

Kosheleva, R. I., Mitropoulos, A. C., & Kyzas, G. Z. (2019). Synthesis of activated carbon from food waste. *Environmental Chemistry Letters*, *17*(1), 429–438. https://doi.org/10.1007/s10311-018-0817-5

Li, X., Wang, Y., Zhang, G., Sun, W., Bai, Y., Zheng, L., Han, X., & Wu, L. (2019). Influence of Mg-promoted Ni-based Catalyst Supported on Coconut Shell Carbon for CO2 Methanation. *ChemistrySelect*, *4*(3), 838–845. https://doi.org/10.1002/slct.201803369

Lu, Y., & Li, S. (2019). Preparation of Hierarchically Interconnected Porous Banana Peel Activated Carbon for Methylene Blue Adsorption. *Journal Wuhan University of Technology, Materials Science Edition*, *34*(2), 472–480. https://doi.org/10.1007/s11595-019-2076-0

Manojkumar, R., Haranethra, S., Muralidharan, M., & Ramaprabhu, A. (2021). I.C. Engine emission reduction using catalytic converter by replacing the noble catalyst and using copper oxide as the catalyst. *Materials Today: Proceedings*, *45*), 769–773. https://doi.org/10.1016/j.matpr.2020.02.804

Méndez, A., Álvarez, M. L., Fidalgo, J. M., Di Stasi, C., Manyà, J. J., & Gascó, G. (2022a). Biomass-derived activated carbon as catalyst in the leaching of metals from a copper sulfide concentrate. *Minerals Engineering*, *183*(April), 107594. https://doi.org/10.1016/j.mineng.2022.107594

Méndez, A., Álvarez, M. L., Fidalgo, J. M., Di Stasi, C., Manyà, J. J., & Gascó, G. (2022b). Biomass-derived activated carbon as catalyst in the leaching of metals from a copper sulfide concentrate. *Minerals Engineering*, *183*(October 2021). https://doi.org/10.1016/j.mineng.2022.107594

Naveenkumar, R., Ramesh Kumar, S., Pushyanthkumar, G., & Senthil Kumaran, S. (2020). NOx, CO & HC control by adopting activated charcoal enriched filter in catalytic converter of diesel engine. *Materials Today: Proceedings*, *22*, 2283–2290. https://doi.org/10.1016/j.matpr.2020.03.349

Neme, I., Gonfa, G., & Masi, C. (2022). Preparation and characterization of activated carbon from castor seed hull by chemical activation with H3PO4. *Results in Materials*, *15*(June), 100304. https://doi.org/10.1016/j.rinma.2022.100304

Neolaka, Y. A. B., Lawa, Y., Naat, J., Riwu, A. A. P., Darmokoesoemo, H., Widyaningrum, B. A., Iqbal, M., & Kusuma, H. S. (2021). Indonesian Kesambi wood (Schleichera oleosa) activated with pyrolysis and H2SO4 combination methods to produce mesoporous activated carbon for Pb(II) adsorption from aqueous solution. *Environmental Technology and Innovation*, *24*, 101997. https://doi.org/10.1016/j.eti.2021.101997

Nguyen, D. T. C., Nguyen, T. T., Le, H. T. N., Nguyen, T. T. T., Bach, L. G., Nguyen, T. D., Vo, D. V. N., & Van Tran, T. (2021). The sunflower plant family for bioenergy, environmental remediation, nanotechnology, medicine, food and agriculture: a review. *Environmental Chemistry Letters*, *19*(5), 3701–3726. https://doi.org/10.1007/s10311-021-01266-z

Nikić, J., Tubić, A., Watson, M., Maletić, S., Šolić, M., Majkić, T., & Agbaba, J. (2019). Arsenic removal from water by green synthesized magnetic nanoparticles. *Water (Switzerland)*, *11*(12). https://doi.org/10.3390/w11122520

Nofendri, Y. (2019). Pengaruh Penambahan Oksigenat Pada Solar Terhadap Emisi Gas Buang Mesin Diesel. *Jurnal Kajian Teknik Mesin*, *3*(1), 30–39. https://doi.org/10.52447/jktm.v3i1.1592

Nugraha, R. E., Prasetyoko, D., Asikin-Mijan, N., Bahruji, H., Suprapto, S., Taufiq-Yap, Y. H., & Jalil, A. A. (2021). The effect of structure directing agents on micro/mesopore structures of aluminosilicates from Indonesian kaolin as deoxygenation catalysts. *Microporous and Mesoporous Materials*, *315*(October 2020), 110917. https://doi.org/10.1016/j.micromeso.2021.110917

Oyim, J., Amuhaya, E., Matshitse, R., Mack, J., & Nyokong, T. (2022). Integrated photocatalyst adsorbents based on porphyrin anchored to activated carbon granules for water treatment. *Carbon Trends*, *8*, 100191. https://doi.org/10.1016/j.cartre.2022.100191

Presin Kumar, J., Sivakumar, S., Balaji, R., Sathish, S., & Nadarajan, M. (2019). Effective Utilization of Banana Plant Waste Materials for Catalytic Converter Filter in Kirloskar Diesel Engine. *Materials Today: Proceedings*, *24*, 2174–2184. https://doi.org/10.1016/j.matpr.2020.03.675

Pullas Navarrete, J., & de la Torre, E. (2022). Preparation of Activated Carbon Fibers (Acf) Impregnated with Silver Microparticles from Cotton-Woven Wastes and its Performance as an Antibacterial Agent. *SSRN Electronic Journal*, *33*(May), 104598. https://doi.org/10.2139/ssrn.4132020

Rajakrishnamoorthy, P., Karthikeyan, D., & Saravanan, C. G. (2020). Emission reduction technique applied in SI engines exhaust by using zsm5 zeolite as catalysts synthesized from coal fly ash. *Materials Today: Proceedings*, *22*, 499–506. https://doi.org/10.1016/j.matpr.2019.08.097

Ramesh, A., Jeyavelan, M., Rajju Balan, J. A. A., Srivastava, O. N., & Leo Hudson, M. S. (2021). Supercapacitor and room temperature H, CO2 and CH4 gas storage characteristics of commercial nanoporous activated carbon. *Journal of Physics and Chemistry of*

A.Hamid et al

Int. J. Renew. Energy Dev 2023, 12(1), 144-154

| 154

Solids, *152*(September 2020), 109969. https://doi.org/10.1016/j.jpcs.2021.109969

Ratan, J. K., Kaur, M., & Adiraju, B. (2018). Synthesis of activated carbon from agricultural waste using a simple method: Characterization, parametric and isotherms study. *Materials Today: Proceedings*, *5*(2), 3334–3345. https://doi.org/10.1016/j.matpr.2017.11.576

Rawal, S., Joshi, B., & Kumar, Y. (2018). Synthesis and characterization of activated carbon from the biomass of Saccharum bengalense for electrochemical supercapacitors. *Journal of Energy Storage*, *20*(July), 418–426. https://doi.org/10.1016/j.est.2018.10.009

Rodríguez-Sánchez, S., Díaz, P., Ruiz, B., González, S., Díaz-Somoano, M., & Fuente, E. (2022). Food industrial biowaste-based magnetic activated carbons as sustainable adsorbents for anthropogenic mercury emissions. *Journal of Environmental Management*, *312*(February). https://doi.org/10.1016/j.jenvman.2022.114897

Saleh, T. A. (2018). Simultaneous adsorptive desulfurization of diesel fuel over bimetallic nanoparticles loaded on activated carbon. *Journal of Cleaner Production*, *172*, 2123–2132. https://doi.org/10.1016/j.jclepro.2017.11.208

Sethia, G., & Sayari, A. (2016). Activated carbon with optimum pore size distribution for hydrogen storage. *Carbon*, *99*, 289–294. https://doi.org/10.1016/j.carbon.2015.12.032

Shu, J., Cheng, S., Xia, H., Zhang, L., Peng, J., Li, C., & Zhang, S. (2017). Copper loaded on activated carbon as an efficient adsorbent for removal of methylene blue. *RSC Advances*, *7*(24), 14395–14405. https://doi.org/10.1039/c7ra00287d

Soleimani, M., & Kaghazchi, T. (2014). Low-Cost Adsorbents from Agricultural By- Products Impregnated with Phosphoric Acid. *Advanced Chemical Engineering Research*, *3*. www.seipub.org/acer

Soliman, A. M., Alshamsi, D., Murad, A. A., Aldahan, A., Ali, I. M., Ayesh, A. I., & Elhaty, I. A. (2022). Photocatalytic removal of nitrate from water using activated carbon-loaded with bimetallic Pd-Ag nanoparticles under natural solar radiation. *Journal of Photochemistry and Photobiology A: Chemistry*, *433*(April), 114175. https://doi.org/10.1016/j.jphotochem.2022.114175

Sugavaneswaran, M., Rajesh, N., Katta, V., Sathish Kumar, G., & Prakash, R. (2019). Deep Drawing Simulation Study for Catalytic Converter Housing Sheet. *Materials Today: Proceedings*, *22*, 1326–1332. https://doi.org/10.1016/j.matpr.2020.01.425

Sujiono, E. H., Zabrian, D., Zurnansyah, Mulyati, Zharvan, V., Samnur, & Humairah, N. A. (2022). Fabrication and characterization of coconut shell activated carbon using variation chemical activation for wastewater treatment application. *Results in Chemistry*, *4*, 100291. https://doi.org/10.1016/j.rechem.2022.100291

Sujiono, E. H., Zurnansyah, Zabrian, D., Dahlan, M. Y., Amin, B. D., Samnur, & Agus, J. (2020). Graphene oxide based coconut shell waste: synthesis by modified Hummers method and characterization. *Heliyon*, *6*(8), e04568. https://doi.org/10.1016/j.heliyon.2020.e04568

Tonoya, T., Matsui, Y., Hinago, H., & Ishikawa, M. (2022). Microporous activated carbon derived from azulmic acid precursor with high sulfur loading and its application to lithium-sulfur battery cathode. *Electrochemistry Communications*, *140*(August), 107333. https://doi.org/10.1016/j.elecom.2022.107333

Tran, T. Van, Nguyen, D. T. C., Nguyen, T. T. T., Nguyen, D. H., Alhassan, M., Jalil, A. A., Nabgan, W., & Lee, T. (2023). A critical review on pineapple (Ananas comosus) wastes for water treatment, challenges and future prospects towards circular economy. *Science of The Total Environment*, *856*(July 2022), 158817. https://doi.org/10.1016/j.scitotenv.2022.158817

Tripathi, M., Sahu, J. N., & Ganesan, P. (2016). Effect of process parameters on production of biochar from biomass waste through pyrolysis: A review. *Renewable and Sustainable Energy Reviews*, *55*, 467–481. https://doi.org/10.1016/j.rser.2015.10.122

Udhayakumar, N., Ramesh Babu, S., Bharathwaaj, R., & Sathyamurthy, R. (2021). An experimental study on emission characteristics in compression ignition engine with silver and zinc coated catalytic converter. *Materials Today: Proceedings*, *47*, 4959–4964. https://doi.org/10.1016/j.matpr.2021.04.314

Vembathu Rajesh, A., Mathalai Sundaram, C., Sivaganesan, V., Nagarajan, B., & Harikishore, S. (2020). Emission reduction techniques in CI engine with catalytic converter. *Materials Today: Proceedings*, *21*, 98–103. https://doi.org/10.1016/j.matpr.2019.05.369

Venkatesan, S. P., Uday, D. S., Hemant, B. K., Kushwanth Goud, K. R., Kumar, G. L., & Kumar, K. P. (2017). I.C. Engine emission reduction by copper oxide catalytic converter. *IOP Conference Series: Materials Science and Engineering*, *197*(1). https://doi.org/10.1088/1757-899X/197/1/012026

Waly, S. M., El-Wakil, A. M., El-Maaty, W. M. A., & Awad, F. S. (2021). Efficient removal of Pb(II) and Hg(II) ions from aqueous solution by amine and thiol modified activated carbon. *Journal of Saudi Chemical Society*, *25*(8), 101296. https://doi.org/10.1016/j.jscs.2021.101296

Zhang, G., Liu, H., Liu, R., & Qu, J. (2009). Adsorption behavior and mechanism of arsenate at Fe-Mn binary oxide/water interface. *Journal of Hazardous Materials*, *168*(2–3), 820–825. https://doi.org/10.1016/j.jhazmat.2009.02.137

Zhang, S., Zeng, M., Xu, W., Li, J., Li, J., Xu, J., & Wang, X. (2013). Polyaniline nanorods dotted on graphene oxide nanosheets as a novel super adsorbent for Cr(vi). *Dalton Transactions*, *42*(22), 7854–7858. https://doi.org/10.1039/c3dt50149c